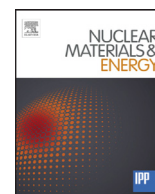


Contents lists available at [ScienceDirect](http://ScienceDirect)

# Nuclear Materials and Energy

journal homepage: [www.elsevier.com/locate/nme](http://www.elsevier.com/locate/nme)

## Damage production in atomic displacement cascades in beryllium

V.A. Borodin<sup>a,b</sup>, P.V. Vladimirov<sup>c,\*</sup><sup>a</sup> NRC Kurchatov Institute, Kurchatov Sq. 1, 123182 Moscow, Russia<sup>b</sup> NRNU MEPhI, Kashirskoe Sh. 31, 115409 Moscow, Russia<sup>c</sup> Karlsruhe Institute of Technology, Karlsruhe, Germany

### ARTICLE INFO

Article history:  
Available online xxx

Keywords:  
Beryllium  
Cascade  
Simulation  
Molecular dynamics

### ABSTRACT

The paper presents the results of a molecular dynamics simulation of cascade damage production in beryllium caused by self-ion recoils in the energy range of 0.5–3 keV. It is demonstrated that point defects are produced in Be preferentially in well-separated subcascades generated by secondary and higher order recoils. A linear dependence of the point defect number on the primary recoil energy is obtained with the slope that corresponds to formal atom displacement energy of ~21 eV. Most of the damage is created as single defects and the relatively high part of created point defects (~50%) survives the correlated recombination following the ballistic cascade stage and becomes freely-migrating.

© 2016 Published by Elsevier Ltd.

This is an open access article under the CC BY-NC-ND license (<http://creativecommons.org/licenses/by-nc-nd/4.0/>).

### 1. Introduction

Beryllium is an important functional material for future fusion devices. Metallic beryllium in the form of small spherical particles (pebbles) is considered as a neutron multiplication material in the fusion reactor blanket. Fast neutrons are known to produce in Be considerable amounts of both point defects and transmutation gases, which can have detrimental effect on the microstructure and mechanical properties of Be pebbles (see e.g. [1]). Mobile self-defects (interstitials, vacancies and small clusters thereof) contribute to various undesirable secondary effects, such as the formation of large point defect clusters (dislocation loops, voids, gas bubbles) both inside the grain and on grain boundaries, the segregation of dopants at grain boundaries and interfaces, etc. Theoretical predictions of the microstructural development kinetics are impossible without the knowledge of the efficiency of primary damage production by irradiation.

When fast neutrons penetrate a solid, they create considerable amounts of fast primary recoil atoms, which, in turn, create radiation damage. For a rough estimate of the number  $N$  of atomic displacements created by a primary recoil that has got an initial energy  $E$ , one often applies the Norgett–Robinson–Torrens (NRT) [2] relation

$$N_{\text{NRT}} = 0.8 \frac{E}{2E_d}, \quad (1)$$

where  $E_d$  is the threshold energy for atom displacement. Unfortunately, the reliability of predictions using Eq. (1) is relatively low for a number of well-known reasons. First of all, the equation was derived assuming that the scattering of primary and higher order recoils can be described in the framework of the binary collision approximation (BCA). Subsequent investigations have demonstrated that BCA is inapplicable to recoils with relatively low (one to tens keV) projectile energies, which create damage in dense collision cascades, where many atomic collisions occur in a strongly correlated mode. Second, the exact value of the threshold displacement energy is only seldom known from experimental measurements and is quite hard to estimate numerically (e.g. [3]), so one has to use rule of thumb estimates (e.g.  $E_d = 25$  eV for Be [4]). Third, thermal effects on post-ballistic cascade stage, such as correlated recombination of interstitials and vacancies in localized cascade area, are able to significantly reduce the number of point defects able to escape into the bulk and participate in the secondary damage creation. Hence, the common application of BCA-based numerical codes (such as SRIM [4]) for the estimation of the amount of neutron damage (e.g. Ref. [5] for Be) provides at best an order of magnitude estimate due to the improper description of low-energy collision cascades.

In order to improve the numerical evaluation of damage by collision cascades, it is a common practice to apply molecular dynamics (MD). One can find in the literature detailed MD simulations of collision cascades in various materials (see e.g. [6,7]). However, to the best of our knowledge, no MD studies of cascade damage production have been published for beryllium. Here we report some results of a MD investigation of point defect

\* Corresponding author.

E-mail address: [pavel.vladimirov@kit.edu](mailto:pavel.vladimirov@kit.edu) (P.V. Vladimirov).<http://dx.doi.org/10.1016/j.nme.2016.07.001>2352-1791/© 2016 Published by Elsevier Ltd. This is an open access article under the CC BY-NC-ND license (<http://creativecommons.org/licenses/by-nc-nd/4.0/>).

production and intra-cascade annealing in cascades caused in Be by fast self-ions.

## 2. Simulation technique

The simulations were performed using the LAMMPS code [8]. The interatomic forces are described with the atomic bond-order potential (ABOP) developed in Ref. [9], which is currently the only potential able to reliably reproduce the properties of point defects in Be. Following to the common practice of cascade simulations, at small interatomic distances ( $< 0.8 \text{ \AA}$ ) the potential was smoothly concatenated with the universal repulsive Ziegler–Biersack–Littmark potential [4] in order to prevent unphysically close ion collisions.

The simulation cell used in these calculations had orthorhombic shape with axis  $z$  oriented along the  $c$ -axis of hcp beryllium lattice, while  $x$  and  $y$  axes were along  $\langle 1\bar{1}00 \rangle$  and  $\langle 11\bar{2}0 \rangle$  directions, respectively. The simulation cell size was  $184 \times 159.3 \times 180.8 \text{ \AA}$ . The interatomic distance in the basal plane was  $2.3 \text{ \AA}$  and  $c/a$  ratio – 1572. The simulation cell contained  $\sim 6.4 \times 10^5$  lattice sites. Periodic boundary conditions were applied along all three axis directions.

Before starting cascade simulations, the lattice was pre-heated to 600 K and equilibrated at this temperature. To launch a cascade, the momentum of one of the atoms was replaced with that corresponding to the desired primary recoil energy and oriented randomly in space. In this way, ten cascades at each energy were initiated. The temperature during the simulation runs was maintained using the Berendsen thermostat [10], except for the first 2 ps of each run, where thermostatting was switched off in order not to involve small artificial damping of strongly excited target atoms at the ballistic cascade stage. After the termination of the ballistic stage, a two-stage temperature control scheme was applied in order to simulate the intra-cascade defect annealing. At the first stage the simulation cell was kept at 600 K for 500–750 ps. The temperature of 600 K, a typical one for standard nuclear reactors, is high enough to promote quick diffusion of Be interstitials and the correlated recombination at post-ballistic stage. Often this was sufficient in order to reach the state, when no interstitial-vacancy pair was separated by less than a certain cutoff ('maximum recombination distance'), selected here to be  $12 \text{ \AA}$ . If this was not the case, the simulations were continued at elevated temperature (800 K) in order to accelerate the interstitial diffusion.

The time step for the MD simulation was 0.04–0.05 fs (depending on recoil energy) for the first 2 picoseconds and then switched to 1 fs.

Electronic stopping in the form of the velocity-proportional friction force was taken into account at the stage of the primary recoil deceleration. However, after the recoil redistributed its energy between the lattice atoms, the friction forces become negligible (e.g.  $\sim (3\text{--}5) \times 10^{-9} \text{ eV/\AA}$  for a secondary recoil with the kinetic energy of 10–20 eV, assuming the friction coefficient of  $2.16 \times 10^{-5} \text{ amu/ps}$  for Be ion in Be target [4]), so electronic stopping was switched off after the termination of the ballistic stage.

Particular attention was paid to the selection of the maximum primary energy compatible with the used simulation cell size. Indeed, too fast recoils can cross simulation cell boundary and, together with sufficiently fast secondary recoils, initiate cascades extending over more than one simulation cell. Due to the periodic boundary conditions, this can result in the overlapping of cascade parts belonging to different periodic images of the simulation cell, making the predictions of the point defect production and annealing senseless. Hence, several test cascades with primary recoil energies up to 10 keV (a typical energy for similar simulation cells in such metals as iron or copper [7]) were simulated. As illustrated in Fig. 1, even at comparatively low energies of several keV Be ions are able to travel relatively large distances, noticeably

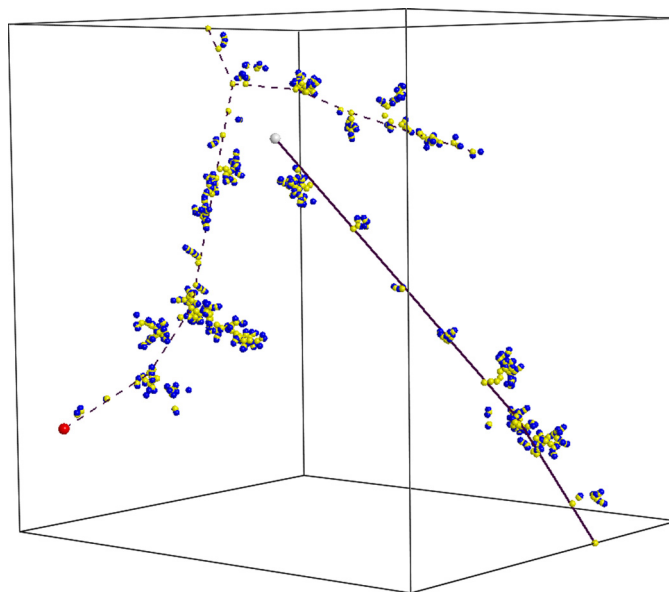


**Fig. 1.** An example of the subcascade mode of primary damage production by a 5 keV recoil ion. The snapshot corresponds to 150 fs simulation time, that is in the middle of the ballistic stage. Strongly displaced atoms and vacancies are shown as dark and light (blue and yellow in colour version) spheres, respectively. Even though the primary recoil is already stopped, at least one secondary ion, shown with a larger dark (red) sphere is sufficiently fast to propagate farther in the ballistic mode. The cascade backbone (i.e. the approximate trajectories of the primary and sufficiently fast secondary recoils) is marked by black lines; the lines corresponding to the cascade part propagating in the image simulation cell are dashed. The vacancy left by the primary recoil (i.e. its starting position) is shown as a larger white sphere. (For interpretation of the references to colour in this figure legend, the reader is referred to the web version of this article.)

exceeding the simulation cell size. Hence, the systematic cascade modeling was undertaken only for primary recoil energies  $\leq 3 \text{ keV}$ . Strictly speaking, later simulations have demonstrated that, in spite of quite large simulation cell size used here, only recoils with the initial energy  $< 2 \text{ keV}$  always remained completely within the simulation cell. At larger energies (occasionally even at 2 keV), the primary recoils tended to cross the cell boundary and continued their motion in an image cell. However, as far as the initial recoil energy did not exceed 3 keV, the parts of recoil trajectory in the main and the image cells were usually well separated and the point defects created along these trajectory parts did not interact during subsequent annealing (which was always checked), so the defect annealing statistics was not distorted.

As can be noticed in Fig. 1, the propagation of fast Be ion in a beryllium target occurs in the so-called 'subcascade' regime. That is, the projectile trajectory remains nearly straight for many interatomic distances before the projectile experiences sufficiently strong scattering on a target atom. Such knocked-on target atoms (secondary recoils) produce either subcascades (well localized damage regions where point defects are produced via collective motion of many atoms), or, if fast enough, also propagate in the subcascade regime.

The lower boundary for the primary recoil energy was taken equal to 0.5 keV because at lower energies the damage is created primarily in the form of individual Frenkel pairs or small defect clusters.

In order to visualize point defects and their clusters, the raw MD data were post-processed using the extended Lindemann technique [11]. The method identifies vacant sites and displaced lattice atoms by surrounding all lattice sites with spheres of small radius ('Lindemann spheres') and postulating that the sites that contain no atoms in their Lindemann spheres are vacant. Correspondingly, strongly displaced are those atoms that do not fall in-

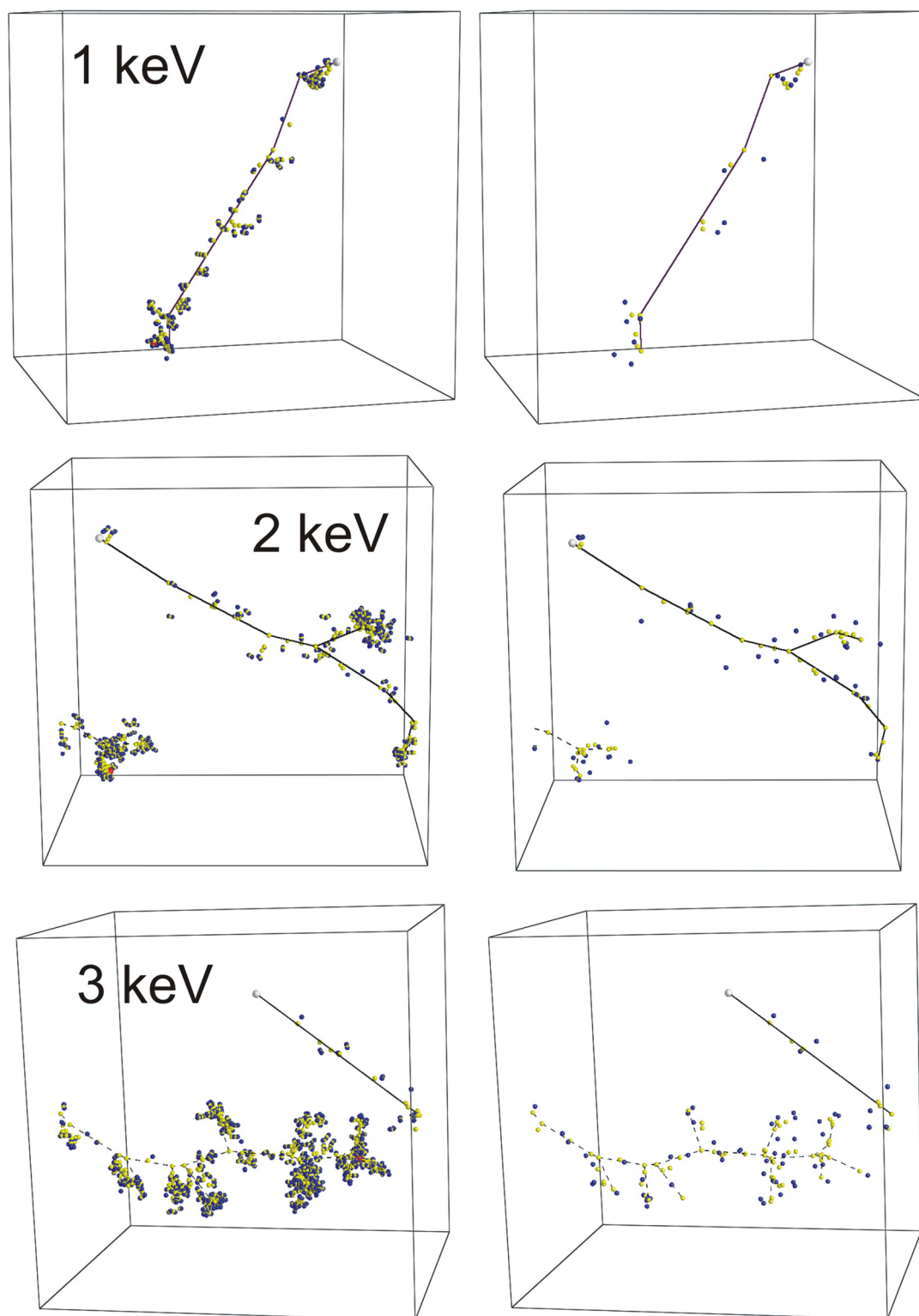


**Fig. 2.** Comparison of cascades at different primary recoil energies, both close to the peak damage production (left row) and after the end of ballistic stage (right row). The recoil energies for each row are indicated in the figure. Defect presentation and colouring scheme is the same as in Fig. 1.

side any Lindemann sphere. Here the Lindemann sphere radius was taken equal to  $0.7 \text{ \AA}$ .

### 3. Results

The cascade dynamics in the current simulation can be separated into two stages. At the first (ballistic) stage, the primary fast

recoil generates dynamically multiple atomic displacements. The stage is very short; the peak damage is reached within  $0.5\text{--}0.8 \text{ ps}$ , while the ballistic movement of target atoms stops at  $0.8\text{--}1.2 \text{ ps}$ , depending on the primary recoil energy. Approximately  $1 \text{ ps}$  more is required for the thermal equilibration of the remaining damage zones.

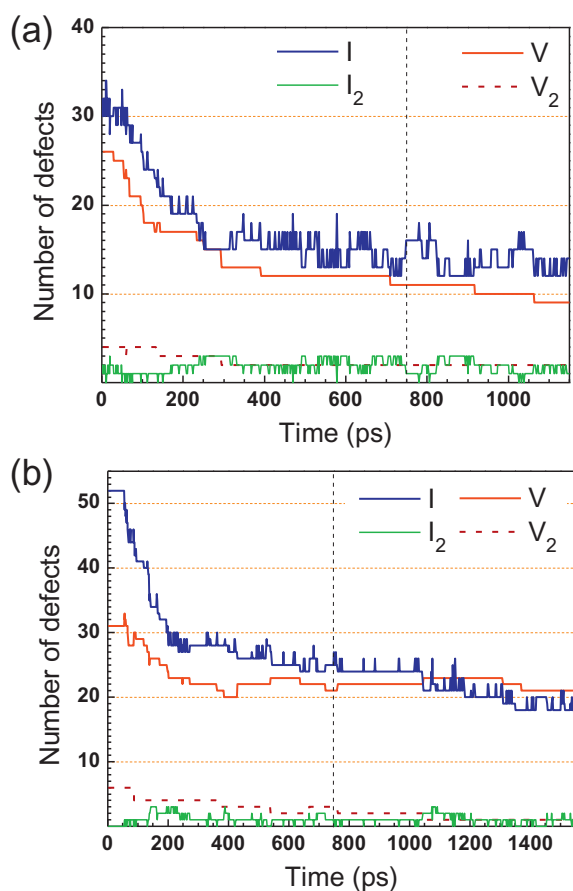


**Fig. 3.** The numbers of interstitials ( $I$ ), di-interstitials ( $I_2$ ), vacancies ( $V$ ) and divacancies ( $V_2$ ) as a function of annealing time for two selected cascades produced by either 2 keV (a) or 3 keV (b) primary recoils. Line color correspondence to defect types and sizes is explained in the legend.

Typical samples of cascades at different primary recoil energies are shown in Fig. 2. One can easily notice that even at relatively low primary recoil energies the damage is produced in the ‘sub-cascade’ regime. Only at the end of range the primary recoil contributes strongly to the total damage creating its own subcascade. Such mode of damage creation resulted in a specific spatial distribution of the damage after the end of ballistic stage; vacancies mostly decorated the cascade backbone, while interstitials were in small clouds at the ends of secondary and higher order trajectory branches.

After the ballistic stage was over, the second stage of the intra-cascade annealing of closely separated vacancies and interstitials started. To be specific, the second stage was assumed here to start at 3 ps.

Two typical examples of the correlated damage annealing are shown in Fig. 3. The major mode of damage annealing is the interstitial-vacancy recombination. It is due exclusively to interstitial-type defects that are mobile at 600 K, while vacancy jumps, though possible, are extremely rare at the simulation time scale. Remarkable is the relatively large recombination radius, which can reach 1 nm. After some time ( $\sim 300$  ps) the recombination nearly cancels out, because nearly all remaining interstitial defects move sufficiently far away from the recoil trajectory, where vacancies are concentrated.

It can also be seen in Fig. 3 that the major part of interstitials is in single defects. Interstitial-interstitial collisions are infrequent, though regular, but di-interstitials move even faster than single interstitials and have rather high probability to recombine with the

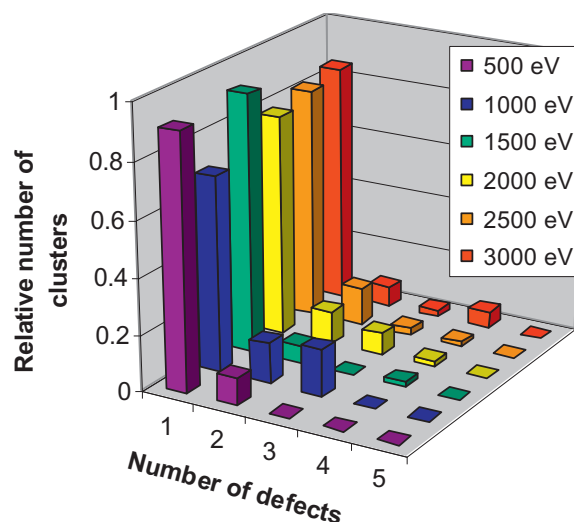


**Fig. 4.** The distribution of interstitial defects over sizes after long-term annealing for different recoil energies. Each bar gives the relative share of interstitials in clusters of particular size.

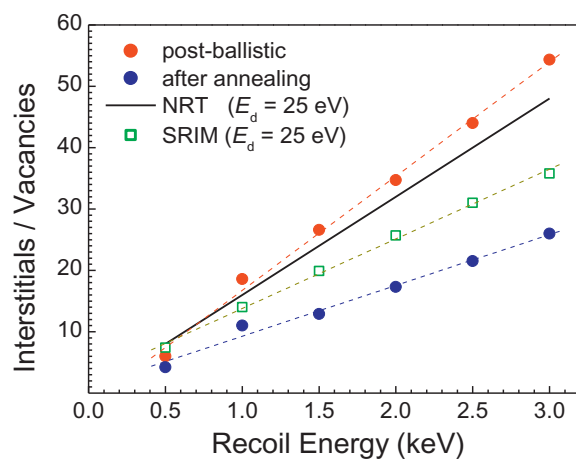


**Fig. 5.** The predicted numbers of Frenkel pairs after the ballistic and annealing stages vs. the primary recoil energy. For comparison, the predictions of Eq. (1) and SRIM code are shown, assuming the displacement threshold energy of 25 eV. The dash lines are linear fits to corresponding data.

vacancies dispersed along the primary recoil trajectory. The final average size distributions of interstitial defects after the end of correlated recombination stage are shown in Fig. 4. The figure confirms that the absolute majority of interstitial defects leaving the cascade region are single interstitials. A relatively low share of di- and tri-interstitials (which are mobile in Be) can also contribute to freely-migrating defects.

All vacancy clusters in the current simulations (i.e. rare di- and tri-vacancies) were produced already at the ballistic stage. A part of them was removed during the intra-cascade annealing. While vacancy clustering in the cascade zone can be expected after the end of the correlated recombination stage, it is too slow to be followed by MD.

Finally, Fig. 5 shows the variation of the total number of Frenkel pairs after the ballistic and annealing stages as a function of the primary recoil energy. As can be seen, the number of pairs generated at the ballistic stage is very similar to predictions of Eq. (1) with the standard displacement energy for beryllium of  $E_d = 25$  eV [4]. In fact, the simulation results would be reproduced exactly using a slightly lower value of  $E_d \approx 21$  eV. Interestingly, a similar dependence obtained using Monte-Carlo code SRIM

[4] predicts (when applying the full-cascade calculation regime) less damage production than either the current simulations or the NRT equation for the same displacement threshold of 25 eV.

In the whole investigated range of primary recoil energies, the linear variation of created point defect numbers with the recoil energy is observed. This seems to be a common feature for 'low-Z' materials, where the cascades are quite extended even at relatively low initial recoil energies (cf., for example, the results for Si [6,11]). In contrast, in heavier metals (Fe, Cu) one often observes a sub-linear dependence in the range of projectile energies up to a certain threshold (typically  $\sim 10$  keV), where compact cascades are predominantly produced [7,12,13].

After the end of the correlated recombination stage, the linear dependence of the Frenkel pair number on the primary recoil energy persists, but the absolute value of the remaining defects is approximately half of that created at the ballistic stage.

#### 4. Summary

Summing up, damage production by fast self-ions in beryllium is markedly different from that in more heavy metals. Even at relatively low primary recoil energies the displaced atoms are produced in the subcascade regime. As a result, the primary recoil trajectories are very long. The vacancies and interstitials decorate the cascade backbone, which is very different from the observations in heavier metals, where vacancies tend to form relatively compact core surrounded by a shell of interstitials. Due to the specific spatial arrangement of point defects, the correlated recombination within the cascades is very efficient, eliminating half of the

primary damage. The interstitial defects that eventually escape from the cascade region into the bulk are nearly exclusively highly mobile single interstitials.

#### Acknowledgements

The authors are grateful to the Steinbuch Computer Center (KIT, Karlsruhe) and the Computer Center of NRC Kurchatov Institute (Moscow) for the use of their computational facilities. One of the authors (VB) acknowledges the financial support for his working stays at KIT from the KIT Fusion Program.

#### References

- [1] V. Chakin, A.O. Posevin, R.N. Latypov, *Atom. Energy* 101 (2006) 743.
- [2] M.J. Norgett, M.T. Robinson, I.M. Torrens, *Nucl. Eng. Des.* 33 (1975) 50.
- [3] K. Nordlund, J. Wallenius, L. Malerba, *Nucl. Instr. Meth. Phys. Res. B* 246 (2006) 322.
- [4] J.F. Ziegler, J.P. Biersack, U. Littmark, *The Stopping and Range of Ions in Matter*, Pergamon, New York, 1985 <http://www.srim.org>.
- [5] T. Troev, N. Nankov, L. Petrov, E. Popov, *Res. Lett. Phys.* 2008 (2008) 746892.
- [6] K. Nordlund, M. Ghaly, R.S. Averback, M. Caturla, T. Diaz de la Rubia, J. Tarus, *Phys. Rev. B* 57 (1998) 7556.
- [7] D.J. Bacon, Yu.N. Osetsky, R. Stoller, R.E. Voskoboynikov, *J. Nucl. Mater.* 323 (2003) 152.
- [8] S. Plimpton, *J. Comp. Phys.* 117 (1995) 1 <http://lammps.sandia.gov>.
- [9] C. Björkas, N. Juslin, H. Timko, K. Vörtler, K. Nordlund, K. Henriksson, P. Erhart, *J. Phys.* 21 (2009) 445002.
- [10] H.J.C. Berendsen, J.P.M. Postma, W.F. van Gunsteren, A. DiNola, J.J.R. Haak, *Chem. Phys.* 81 (1984) 3684.
- [11] V.A. Borodin, *Nucl. Instr. Meth. Phys. Res. B* 282 (2012) 33.
- [12] R.S. Averback, R. Benedek, K.L. Merkle, *Phys. Rev. B* 18 (1978) 4156.
- [13] R.E. Stoller, *J. Nucl. Mater.* 276 (2000) 22.